Organogels

DOI: 10.1002/anie.200703946

Ultrasound Switch and Thermal Self-Repair of Morphology and Surface Wettability in a Cholesterol-Based Self-Assembly System**

Junchen Wu, Tao Yi, Tianmin Shu, Mengxiao Yu, Zhiguo Zhou, Miao Xu, Yifeng Zhou, Huijun Zhang, Jiantao Han, Fuyou Li, and Chunhui Huang**

Recently, stimuli-responsive low-weight molecular organogels[1] have been the subject of increasing attention in areas ranging from chemistry and biology to materials science for their potential applications, such as drug delivery,[2] mechanical action (for example, triggered changes in shape or size),[3] hydrophilicity/hydrophobicity modulation,[4] optical and electronic effects,[5] and so on. Despite a wide range of reported responsive materials, the mostly used stimuli involve light,[5] reaction,[2] and heat.[6] However, it should be noted that development of a smart or adaptive gel which can be controlled or even switched by sound[7] and thixotropy[8] is also very appealing. The groups of Sijbesma[9] and Naota[7a,c] have contributed the majority of the studies on ultrasound-induced reversible gelation. However, there is still no report on a functionality change or even switch induced by ultrasound stimuli.

The Naota[7a,c] and Zhang[10] groups independently observed ultrasound-induced gelation in hydrogen-bonded gelators for the first time. Taking into account the special distribution of ultrasonic stimuli for gelation, especially for H-bonding gel formation, the judicious design of the H bonds in a different environment and the balance of the H bonds with other interactions such as π···π interactions and hydrophobic interactions, as well as the steric hindrance, are necessary to satisfy the ultrasound-responsive requirements. Herein, we report the design and synthesis of three compounds **1a–c** (Scheme 1) with ALS[11] (aromatic group A, linker L, steroidal group S) structural character, in which a naphthalic unit was used as aromatic group A and cholesterol was used as steroidal group S. The introduction of a fluorophore (naphthalic unit) into such a system is not only applicable to photonic soft materials but also for the facile study of molecular aggregation. These two groups were linked by an alkyl chain with zero (**1a**), one (**1b**), or two (**1c**) acyl amino linkages. Therefore, it can be expected that three kinds of intermolecular interaction, including hydrogen bonding, π···π interactions, and hydrophobic interactions, would be involved in the aggregation of the molecules. These interactions achieve a mutual balance to modulate the packing arrangement of the molecules and the hierarchical superstructures, and thus should offer, at least to some extent, the possibility of controlling the formation of the gel by a specific stimulus. It is exciting that an ultrasonic switch and thermal self-repair of morphology and surface properties has been realized in a self-assembly system. To the best of our knowledge, this is the first example related to ultrasound-induced morphology and surface property changes in a gel system, and this study also provides a strategy for the development of responsive soft materials.

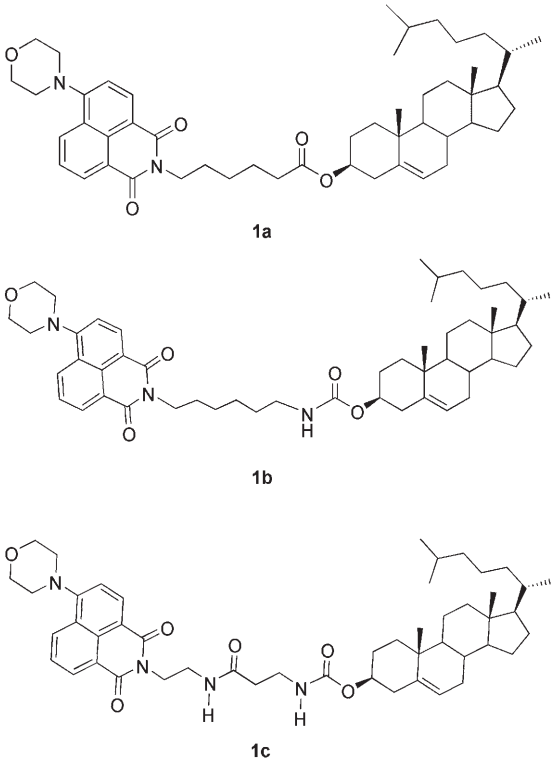

Scheme 1. Chemical structures of **1a–c**.

The synthesis and characterization of **1a–c** are described in the Supporting Information. The gelation abilities of **1a–c** are completely different although the compounds are structurally similar (Table S1 in the Supporting Information).

[*] J. Wu, Dr. T. Yi, T. Shu, M. Yu, Z. Zhou, M. Xu, Y. Zhou, H. Zhang, J. Han, Dr. F. Li, Prof. C. Huang
Department of Chemistry and Laboratory of Advanced Materials
Fudan University, 220 Handan Road, Shanghai 200433 (China)
Fax: (+86) 21-55664621
E-mail: yitao@fudan.edu.cn
chhuang@pku.edu.cn
Homepage: http://www.chemistry.fudan.edu.cn/

[**] This work was supported by the National Science Foundation of China (20571016, 20490210), Shanghai Sci. Tech. Comm. (06J14016), National High Technology Program of China (2006AA03Z318), and Shanghai Leading Academic Discipline Project (B108). The authors greatly appreciate Prof. Erqiang Chen and Dr. Min-qiao Ren (Peking University) for their help on the SAXS analysis.

Supporting information for this article is available on the WWW under http://www.angewandte.org or from the author.

Compound **1a** failed to form gels in a range of organic solvents, irrespective of the solution concentration and ultrasound owing to its high solubility. In contrast, **1b** formed gels in alcohols exclusively upon ultrasonic treatment, while other external stimuli such as quick heating or cooling did not initiate aggregation. The sonicated gel of **1b** was readily converted into the original solution upon heating (80 °C) and was subsequently cooled to room temperature in a moderate concentration (see Figure S1 in the Supporting Information). It is interesting to note that gelation occurred in a variety of solutions of **1c** by ultrasonic treatment (0.16 $W cm^{-2}$, 40 KHz) for several seconds (designated as S gel; Figure S1 b,c in the Supporting Information). To our surprise, **1c** could also form a clear gel by directly cooling the hot solution (above 75 °C) to room temperature and aging for about one hour in *n*-butanol and 30 min in *p*-xylene (designated as T gel). The critical gelation concentration was significantly decreased from 15 $mg mL^{-1}$ (1.8×10^{-2} $mol L^{-1}$) in the cooling process to 10 $mg mL^{-1}$ (1.2×10^{-2} $mol L^{-1}$) in the ultrasonic process for both solvents, and the gel–sol transition temperature (T_g) for the S gel was higher than that for the T gel for the same concentration (Figure S2 in the Supporting Information). At the same time, after undergoing sonication, a reversed gel (R gel) was obtained by heating the S gel to a sol and then cooling it to room temperature. Comparing the gelation ability of the three compounds, it can be concluded that both the amide and carbamate linkages contributed to hydrogen-bond formation and, thus, to the ultrasonic gelation of **1b** and **1c**. As a further result, **1c** can form a gel not only under sonication but also by a thermal process.

The morphologies of xerogels obtained from **1b** and **1c** were investigated by SEM (Figure 1). The **1b** xerogel from *n*BuOH from sonication gives column-like pieces of approximate width 1.0–1.5 μm and approximate length 10–15 μm (Figure 1 a). Interestingly, we found that the morphologies of **1c** xerogels strongly depend on the solvents and external stimuli. The T gel from *n*BuOH shows a burl-like three-dimensional superstructure of 5 to 10 μm in size (Figure 1 b), while tightly arranged one-dimensional tenuous fibers were obtained from the S gel (Figure 1 c). Furthermore, the morphology of such a xerogel from sonication was basically reverted to that of the T xerogel by a sol–gel process (Figure 1 d). In light of the above observation, to confirm the solvent impact on the action of gelation, the morphology of the **1c** xerogel from *p*-xylene was further investigated. Very surprisingly, honeycomb-like three-dimensional multiporous vesicles of about 10-20 μm in diameter were observed in the T gel (Figure 1 e), in which regular holes of about 2 μm in size were distributed on the surface of the spheres. However, the morphology of the **1c** S xerogel from *p*-xylene shows regular papillae of about 5 μm in size, arranged in multilayered circles (Figure 1 f), thus revealing a sharp contrast to the morphology of the T gel. Meanwhile, the porous spherical vesicles could be recovered by a gel-to-sol operation on the S gel (Figure 1 g). Confocal laser scanning microscopy (CLSM) of the xerogel skeleton of **1c** for a certain transection and the corresponding microfluorescent spectral distribution (Figure S3 in the Supporting Information) also proved that the T gel was a hollow sphere with the fluorescent emission only observable at the shell (Figure 1 h). In contrast, the fluorescence was distributed in the whole layer in the S gel (Figure 1 i). The results strongly suggest that the sonication has changed the aggregation action in the process of gelation.

TEM images of **1c** xerogels from *p*-xylene also give important insights into the superstructures. The TEM image of the T gel shows the formation of right-handed helical nanobelts, with a width of about 30–50 nm and a helical pitch of about 150–200 nm (Figure 1 j). Thus, the multiporous spherical structure in the SEM image of the T gel was a result of an intertexture made up of long helical nanobelts. However, the TEM images of the **1c** S gel revealed left-handed helical fiber structures (Figure 1 k), contrary to that of the T gel. To our surprise, the reversibility of the microstructure of the **1c** S gel to the R gel strongly depends on the gel–sol conditions. A complete recovery was observed when heating the S gel at 120 °C for 1 h and re-gelation to an R gel (Figure 1 l); however, the molecular aggregation could not be completely recovered, so that there still existed a small amount of left-handed helical species, when the S gel was heated at less than 100 °C for a short period of time (Figure S5 in the Supporting Information).

The compounds **1a–c** all exhibit similar absorption spectra in solution (see the Supporting Information). Particularly, the maximum absorption in **1c** is located at 388 nm for the solution (5.0×10^{-5} $mol L^{-1}$ in *p*-xylene, $\varepsilon = 1.27 \times 10^4$ $M^{-1} cm^{-1}$) and 375 nm in the gel (1.2×10^{-2} $mol L^{-1}$), irrespective of sonication or

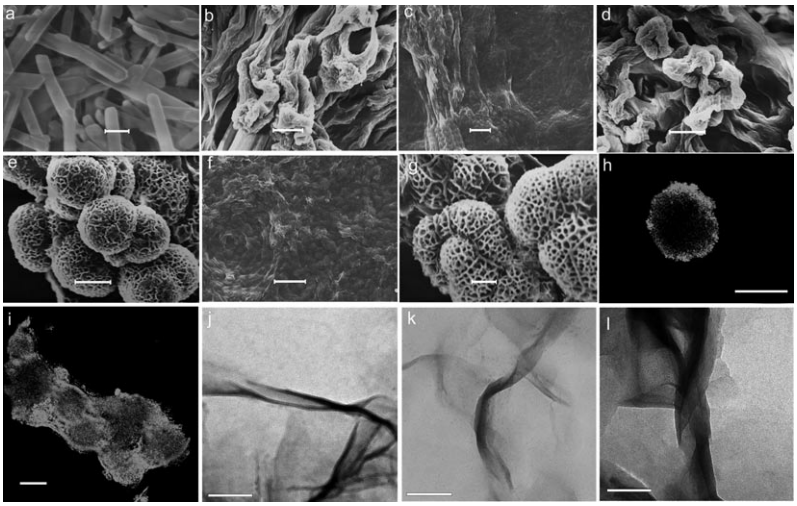

Figure 1. SEM images of the xerogels from the **1b** S gel (a, 30 $mg mL^{-1}$ in *n*-butanol, ultrasonic treatment: 0.16 $W cm^{-2}$, 40 KHz, 5 min); **1c** T gel (b), S gel (c, ultrasonic treatment: 0.16 $W cm^{-2}$, 40 KHz, 30 s), and R gel (d) in *n*-butanol (10 $mg mL^{-1}$); **1c** T gel (e), S gel (f, ultrasonic treatment: 0.16 $W cm^{-2}$, 40 KHz, 30 s), and R gel (g) in *p*-xylene (15 $mg mL^{-1}$). CLSM images of the xerogel skeleton of the **1c** T gel (h) and S gel (i) in *p*-xylene. TEM images of the **1c** T gel (j), S gel (k), and R gel (l) in *p*-xylene. Scale bars: 2 μm (a), 10 μm (b), 5 μm (c), 10 μm (d,e), 20 μm (f), 10 μm (g), 20 μm (h,i), 100 nm (j,k,l).

cooling (Figure S6 in the Supporting Information). The blue-shifted absorption indicated an H aggregation of **1c** molecules in the gel. The emission of **1c** occurred at 515 nm in *p*-xylene solution and was shifted to 508 and 511 nm for the T gel and S gel, respectively (Figure S8 in the Supporting Information). The strong emission of **1c** in the gel provides an appropriate medium for investigating the mechanism. Here, the thermodynamic behavior of the aggregation in a 2.0×10^{-3} mol L^{-1} (1.6 mg mL^{-1}) solution of **1c** in *p*-xylene was investigated. The sample was heated and then cooled to room temperature. The as-prepared solution was quickly divided into two equal-volume samples; the first one was kept at 25 °C while the other was treated by ultrasound (0.16 W cm^{-2}, 40 KHz, 30 s). The aggregation processes of both samples were followed by means of CLSM as a function of time (Figure 2). In this process, the mobile, non-aggregated **1c** in

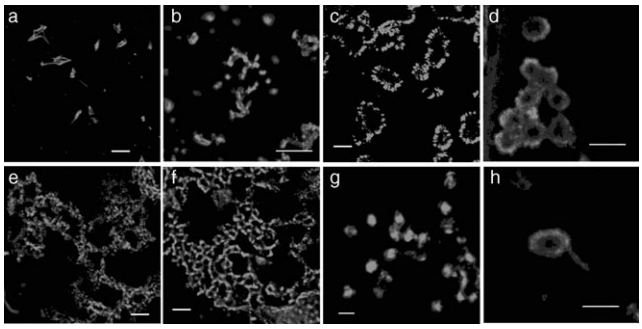

Figure 2. CLSM images of **1c** ($\lambda_{ex}=405$ nm; $\lambda_{em}=450$–550 nm) in xylene: as-prepared solution (a, 2.0×10^{-3} mol L^{-1}), after aging for 6 h (b), 12 h (c), and 24 h (d); as-prepared solution treated with ultrasound (e), after aging for 12 h (f), after subsequent heat–cool process and aging for 12 h (g) and 24 h (h). Scale bars: 5 μm (a), 10 μm (b), 5 μm (c), 10 μm (d), 5 μm (e,f), 2 μm (g), 10 μm (h).

the sol and gel states could be observed as a pronouncedly detectable species similar to conventional gelators. At the beginning, some curly belts of about 2–4 μm in length and 0.5–1 μm in width began to grow out from the as-prepared solution (Figure 2a). After aging for 6 and 12 h, the belts were aggregated and partly integrated to form a semicircular gel skeleton of approximate diameter 5–10 μm (Figure 2b,c). Such aggregation continued and finally gave a spherical skeleton after 24 h of aging (Figure 2d). A kinetic study on the sonicated sample was also carried out (Figure 2a,e–h). The time-dependent CLSM images of **1c** during the entire gelation process indicates that gelation began immediately after sonication, with the small pieces quickly expanding over the whole field (Figure 2e,f). When the sonicated gel was heated to a sol and aged for 12 h at room temperature, small dispersed vesicles with a diameter of 1–2 μm were observed (Figure 2g) and began to join after 24 h of aging to form hollow vesicles of similar size to those observed in Figure 2d (Figure 2h). The above observation suggests that the **1c** segment in the sol tends to form an integral part of the hemisphere gel skeleton rather than a plane network by a thermodynamic process, whereas the sonicated gel consists of an ultrasound-induced initiation step and a subsequent spontaneous propagation step. However, such ultrasound-induced gelation still could be reverted to a conventional gel by a heat–cool control.

The molecular packing of the **1c** xerogel under different external stimuli was further investigated by powder X-ray diffraction spectra (Figure S9 in the Supporting Information). The neat solid of **1c** displays serial peaks at 5.20, 2.75, and 1.73 nm; these values indicate a lamellar structure.[12] The other two dimensions correspond to 1.42 and 0.58 nm, respectively. The T xerogel and S xerogel of **1c** display similar X-ray diffraction profiles, with two peaks corresponding to *d* spacings of 4.07, 1.32 nm and 4.37, 1.42 nm, respectively. The two peaks for the R xerogel correspond to 4.09 and 1.31 nm, similar to those of the T xerogel. It is apparent that the aggregation depends on the gelling stimuli and can be repaired without noticeable changes.

On the basis of the spectral study and XRD results, combined with the CPK model of **1c**, the molecular packing of the xerogels was conjectured as shown in Figure 3. The

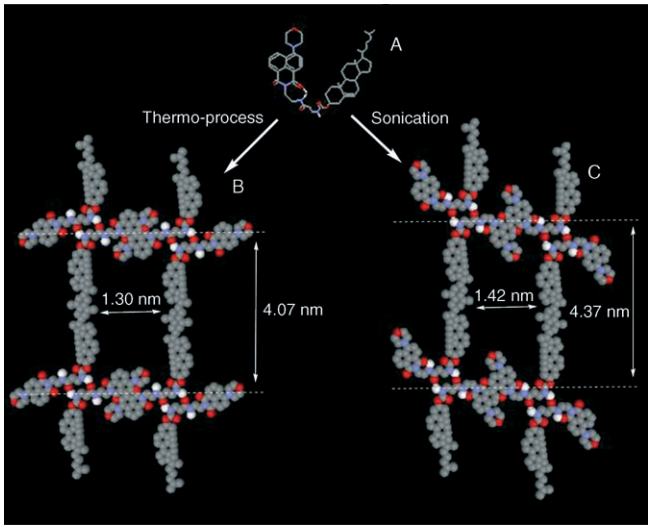

Figure 3. Perspective structures of **1c**; structure A: isolated **1c**; structure B: aggregation in the T gel; structure C: aggregation in the S gel; gray C, red O, blue N. Only hydrogen atoms participating in H bonds are shown as white spheres.

ground-state optimized molecular-geometry calculations (semiempirical AM1 method; see the Supporting Information) and temperature-dependent IR spectra (Figure S10 in the Supporting Information) indicate that the isolated **1c** molecule tends to form a bent conformation by intramolecular hydrogen bonding between the naphthalimide (C=O) and amide (N–H) groups (structure A in Figure 3). The energy difference between the two conformations with and without intramolecular H bonds at ground state is 0.172 eV (69.35 kJ mol^{-1}). However, a bent molecule is not advantageous to gelation in the ALS system;[11c] therefore, in the thermal process, the gradual formation of the intermolecular double H bonds accompanies the disconnection of the intramolecular H bond and unwinds the **1c** molecule (structure B in Figure 3). The molecules are further connected in

the direction perpendicular to the intermolecular H bonds through van der Waals forces between the cholesterol groups with a tilt to the right (P chirality) and a resulting layer distance of 4.07 nm. However, sonication provides heat and pressure on the nanosecond scale and extreme cooling rates,[13] resulting in rapid and spontaneous aggregation through interpenetrating H-bond interactions. As a result, the **1c** molecule does not unwind and maintains the bent conformation in the S-gel state (structure C in Figure 3). This result is different from that described by T. Naota and co-workers in their recent work,[7c] in which the disconnection of the intramolecular H bond by ultrasound and quick formation of an intermolecular H bond were the result of gel formation. The blue shifts in both absorption and emission spectra from solution (including the sol state) to both the T gel and S gel of **1c** indicate a head-to-tail arrangement of the naphthalic groups. The ultrasound-induced instant gelation could also be produced in **1b** because the pressure wave of ultrasound overcomes the steric hindrance and results in regular aggregation of the molecules, which is very similar to what happened in the tetrathiafulvalene compound reported by D. Zhang and co-workers.[10] The observed behavior of the stimuli-responsive self-assembly action greatly increases the potential applicability of these materials for drug delivery and switchable surfaces.

Functional surfaces with controllable wettability have come to the forefront of research for their great potential in biological and industrial applications.[14] These materials possess well-defined micro- and nanostructures on their surfaces. Their wettability can be tuned between hydrophilicity and hydrophobicity by modifying the surface chemistry or topographic structure by various stimuli, including light irradiation,[15] pH change,[16] thermal treatment,[17] and so on. Taking into account the specific morphologies between the **1c** T gel and S gel, the xerogel surface of these gels may possess quite different surface wettability. In fact, when a T xerogel was directly coated onto a glass slice, the film gave a superhydrophobic surface with a contact angle of 159.4° (Figure 4a), whereas the film obtained by the S xerogel gave a contact angle of 104.4° (Figure 4b). Therefore, the surface wettability crucially depends on the gelling action, which can be changed by different external stimuli, such as ultrasound or cooling. Furthermore, the surface of a reversed gel gave a contact angle of 151.3° (Figure 4c). Thus, from T gel to S gel, then to R gel, the wettability of xerogels can be easily modified by ultrasound and recovered by a gel–sol transition, and the cycle can be repeated several times (Figure 4d). To the best of our knowledge, this is the first observation of a reversible ultrasound-induced change in surface morphology and wettability.

In summary, ultrasound-induced gelation in a novel family of asymmetric cholesterol-based fluorescent organogelators was studied. It is surprising that both the self-assembly and surface wettability of the compound with two H-bond sites can be controlled by ultrasound stimuli and restored by a thermal process. A hollow spherical motif was generated in a thermal process. The ultrasound irradiation provides heat and pressure, and thus results in the spontaneous formation of the intermolecular H bonds and aggregation-induced helical motif. We propose that the cooperation and relative competition of intra- and interlinking of the hydrogen bonds, directed by the sonication or thermal process, are the main contributions to the switch. Ultrasound controls regarding the movement and orientation of microscale surface features may have exciting applications in materials for airplanes, biodelivery systems, separation systems, responsive materials, or shape-memory materials. Further studies on these molecules are in progress.

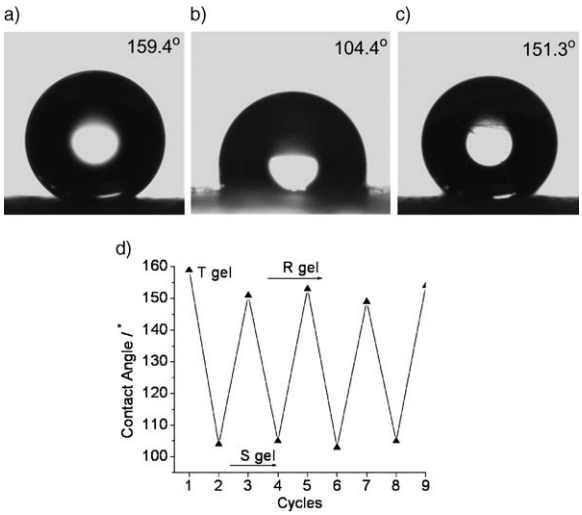

Figure 4. Photographs of the water droplet on glass slices, spin-coated with the **1c** T xerogel (a), S xerogel (b), and R xerogel (c) from *p*-xylene (15 mg mL^{-1}). d) Reversible wettability transition between the T gel and S gel by the sol–gel process.

Received: August 28, 2007
Revised: October 16, 2007
Published online: December 20, 2007

Keywords: gels · helical structure · hydrogen bonds · self-assembly · wettability

[1] a) J. D. Ehrick, S. K. Deo, T. W. Browning, L. G. Bachas, M. J. Madou, S. Daunert, *Nat. Mater.* **2005**, *4*, 298–302; b) J.-M. Lehn, *Polym. Int.* **2002**, *51*, 825–839; c) L. A. Estroff, A. D. Hamilton, *Chem. Rev.* **2004**, *104*, 1201–1218; d) K. J. C. van Bommel, A. Friggeri, S. Shinkai, *Angew. Chem.* **2003**, *115*, 1010–1030; *Angew. Chem. Int. Ed.* **2003**, *42*, 980–999.
[2] J. F. Miravet, B. Escuder, *Org. Lett.* **2005**, *7*, 4791–4794.
[3] a) A. R. Hirst, D. K. Smith, *Chem. Eur. J.* **2005**, *11*, 5496–5508; b) A. R. Hirst, D. K. Smith, J. P. Harrington, *Chem. Eur. J.* **2005**, *11*, 6552–6559.
[4] a) N. Verplanck, E. Galopin, J-C. Camart, V. Thomy, *Nano Lett.* **2007**, *7*, 813–817; b) N. Garcla, E. Benito, J. Guzman, P. Tiemblo, *J. Am. Chem. Soc.* **2007**, *129*, 5052–5060; c) Y. F. Zhou, T. Yi, T. C. Li, Z. G. Zhou, F. Y. Li, W. Huang, C. H. Huang, *Chem. Mater.* **2006**, *18*, 2974–2981.
[5] O. J. Dautel, M. Robitzer, J.-P. Lere-Porte, F. Serein-Spirau, J. J. E. Moreau, *J. Am. Chem. Soc.* **2006**, *128*, 16213–16223.
[6] S.-I. Kawano, N. Fujita, S. Shinkai, *Chem. Eur. J.* **2005**, *11*, 4735–4742.
[7] a) T. Naota, K. Hiroshi, *J. Am. Chem. Soc.* **2005**, *127*, 9324–9325; b) W. Weng, J. B. Beck, A. M. Jamieson, S. J. Rowan, *J.*

Am. Chem. Soc. **2006**, *128*, 11665 – 11672; c) K. Isozaki, H. Takaya, T. Naota, *Angew. Chem.* **2007**, *119*, 2913 – 2915; *Angew. Chem. Int. Ed.* **2007**, *46*, 2855 – 2857.

[8] M. Shirakawa, N. Fujita, S. Shinkai, *J. Am. Chem. Soc.* **2005**, *127*, 4164 – 4165.

[9] a) J. M. J. Paulusse, R. P. Sijbesma, *Angew. Chem.* **2004**, *116*, 4560 – 4562; *Angew. Chem. Int. Ed.* **2004**, *43*, 4460 – 4462; b) J. M. J. Paulusse, D. J. M. van Beek, R. P. Sijbesma, *J. Am. Chem. Soc.* **2007**, *129*, 2392 – 2397; c) J. M. J. Paulusse, J. P. J. Huijbers, R. P. Sijbesma, *Chem. Eur. J.* **2006**, *12*, 4928 – 4934.

[10] C. Wang, D. Q. Zhang, D. B. Zhu, *J. Am. Chem. Soc.* **2005**, *127*, 16372 – 16373.

[11] a) X. Huang, S. R. Raghavan, P. Terech, R. G. Weiss, *J. Am. Chem. Soc.* **2006**, *128*, 15341 – 15352; b) X. Huang, P. Terech, S. R. Raghavav, R. G. Weiss, *J. Am. Chem. Soc.* **2005**, *127*, 4336 – 4344; c) M. George, R. G. Weiss, *Acc. Chem. Res.* **2006**, *39*, 489 – 497.

[12] a) L. A. Estroff, L. Leiserowitz, L. Addadi, S. Weiner, A. D. Hamilton, *Adv. Mater.* **2003**, *15*, 38 – 42; b) K. Hanabusa, M. Matsumoto, M. Kimura, A. Kakehi, H. Shirai, *J. Colloid Interface Sci.* **2000**, *224*, 231 – 244.

[13] a) G. Cravotto, P. Cintas, *Angew. Chem.* **2007**, *119*, 5573 – 5575; *Angew. Chem. Int. Ed.* **2007**, *46*, 5476 – 5478; b) Y. Cai, X. Pan, X. Xu, Q. Hu, L. Li, R. Tang, *Chem. Mater.* **2007**, *19*, 3081 – 3083.

[14] a) T. Sun, L. Feng, X. Gao, L. Jiang, *Acc. Chem. Res.* **2005**, *38*, 644 – 652; b) L. Feng, S. Li, Y. Li, H. Li, L. Zhang, J. Zhai, Y. Song, B. Liu, L. Jiang, D. Zhu, *Adv. Mater.* **2002**, *14*, 1857 – 1860; c) M. Calliea, D. Quéré, *Soft Matter* **2005**, *1*, 55 – 61.

[15] a) R. Wang, K. Hashimoto, A. Fujishima, M. Chikuni, E. Kojima, A. Kitamura, M. Shimohigoshi, T. Watanabe, *Nature* **1997**, *388*, 431 – 432; b) C. Feng, Y. Zhang, J. Jin, Y. Song, L. Xie, G. Qu, L. Jiang, D. Zhu, *Langmuir* **2001**, *17*, 4593 – 4597.

[16] a) X. Yu, Z. Wang, Y. Jiang, F. Shi, X. Zhang, *Adv. Mater.* **2005**, *17*, 1289 – 1293; b) Y. Jiang, Z. Wang, X. Yu, F. Shi, H. Xu, X. Zhang, M. Smet, W. Dehaen, *Langmuir* **2005**, *21*, 1986 – 1990.

[17] T. Sun, G. Wang, L. Feng, B. Liu, Y. Ma, L. Jiang, D. Zhu, *Angew. Chem.* **2004**, *116*, 361 – 364; *Angew. Chem. Int. Ed.* **2004**, *43*, 357 – 360.

